

Flexural behaviour of square UHPC-filled hollow steel section beams

Soner Guler*, Alperen Çopur and Metin Aydoğan

Faculty of Civil Engineering, Istanbul Technical University, 34469, Istanbul, Turkey

(Received December 24, 2011, Revised April 13, 2012, Accepted June 1, 2012)

Abstract. This paper presents an experimental investigation of the flexural behavior of square hollow steel section (HSS) beams subjected to pure bending. Totally six unfilled and nine ultra high performance concrete (UHPC)-filled HSS beams were tested under four-point bending until failure. The effects of the steel tube thickness, the yield strength of the steel tube and the strength of concrete on moment capacity, curvature, and ductility of UHPC-filled HSS beams were examined. The performance indices named relative ductility index (RDI) and strength increasing factor (SIF) were investigated with regard to different height-to-thickness ratio of the specimens. The flexural strengths obtained from the tests were compared with the values predicted by Eurocode 4, AISC-LRFD and CIDECT design codes. The results showed that the increase in the moment capacity and the corresponding curvature is much greater for thinner HSS beams than thicker ones. Eurocode 4 and AISC-LRFD predict the ultimate moment capacity of the all UHPC-filled HSS beams conservatively.

Keywords: concrete-filled hollow steel sections; ultra high performance concrete; flexural behavior; moment capacity; ductility; performance indices; design codes

1. Introduction

Composite members consisting of square steel tubes filled with concrete are widely used in high-rise buildings involving very large applied moments, particularly in zones of high seismicity. Composite square concrete-filled hollow steel sections (HSS) have been used increasingly as columns, beams and beam-columns in braced and un-braced frame structures. The concrete-filled HSS beams that consist of a steel section filled with concrete have many advantages over traditionally reinforced concrete beams. These beams have excellent moment carrying capacity, ductility and stiffness compared with the conventional steel reinforced members. In general, void filling is an effective way to delay premature local buckling and to improve ductility of the hollow steel sections (Gho and Liu 2004).

There have been many studies on the flexural behavior of concrete-filled HSS beams. Lu and Kennedy (1994) performed tests on twelve beams of concrete-filled square and rectangular HSS beams to investigate the effects of different depth to width ratios and different shear span to depth. The test results showed that the ultimate flexural strengths of the composite beams are increased by

*Corresponding author, Ph.D. Student, E-mail: gulersoner@hotmail.com

about 10-30% over that of bare hollow steel sections. Furthermore, the ratio of shear span to depth (a/D) has almost no effect on the flexural strength. Prion and Boehme (1994) conducted four concrete-filled HSS beams with diameter-to-thickness ratio of 89.4 and concrete cylinder strength of 73 MPa. It was found that the concrete-filled HSS beams fail in a very ductile manner.

Elchalakani *et al.* (2001) conducted a series of tests on the flexural behavior of circular concrete-filled HSS beams with D/t ratio between 12 and 110. The results showed that void filling of the steel tube enhances strength, ductility and energy absorption capacity especially for the thinner sections. Varma *et al.* (2002) investigated the flexural force-deformation behavior of the square high strength concrete with 110 MPa compressive strength filled steel tube beam-columns. The results showed that the curvature ductility of the high strength filled steel tube beam-columns decreases significantly with an increase in either the axial load level or the D/t ratio of the steel tube. The yield stress of the steel tube does not seem to have a significant influence on the curvature ductility. The initial section flexural stiffness (K_i) and the serviceability-level section flexural stiffness (K_s) of the concrete-filled HSS beams were defined by Han *et al.* (2004). Chitawadagi and Narasimhan (2009) performed a series of tests on the flexural behavior of circular concrete filled steel tubes under pure bending. Ninety concrete filled steel tube beams were tested with nominal concrete strength of 20, 30 and 40 MPa and with D/t ratio 22.3 to 50.8. The results showed that an increase in the steel tube thickness increases the moment capacity and ductility both of the hollow and concrete-filled hollow steel tubes. Many researchers have investigated the flexural behavior of the concrete-filled hollow steel section beams (Nakamura *et al.* 2004, Kim *et al.* 2006, Kong *et al.* 2007, Shawkat and Fahmy 2008, Soundararajan and Shanmugasundaram 2008, Arivalagan and Kandasamy 2009, Probst *et al.* 2010).

This paper presents an experimental investigation of the flexural behavior of the square UHPC-filled HSS beams. The first aim of this study is to investigate the ultimate moment capacity, the curvature, and the ductility of the UHPC-filled HSS beams with regard to different steel tube thickness. Secondly, the performance indices that represent the increase in moment capacity and ductility are assessed depending on steel tube thickness of the specimens and compared with the results of Chitawadagi and Narasimhan (2009). Finally, the ultimate moment capacities of the composite beams are compared with the design codes such as Eurocode 4 (1994), AISC-LRFD (1999), CIDECT (1995), and Han model (2004).

2. Experimental program

2.1 Concrete properties

Ultra High Performance Concrete (UHPC) was produced by using very fine sand, cement, silica fume, super plasticizers and steel fibers. UHPC is suitable for use in the production of precast elements for civil and structural engineering and architectural applications and can be used for military and strategic structures. UHPC is a highly homogenous composite without coarse aggregates that achieve cube compressive strengths of greater than 150 MPa. In order to achieve the required performance of UHPC, some measures should be taken in the mix design. These are reducing the maximum size of particles for the homogeneity of the concrete, reducing the amount of water-binder ratio in the mix, the use of steel fibers for the ductility, extensive use of the powder materials and fine aggregates, optimum composition of all components and hardening under

Table 1 UHPC mix proportion

	Mix proportions kg (for 1 m ³ concrete)
Cement	1000
Siliceous sand (0.5-2 mm)	250
Siliceous powder (0-0.5 mm)	400
Silica fume	250
Super plasticizer	110
Water	180
OL 6/16 steel fiber	230
ZP 305 Dramix steel fiber	230
Total	2650

pressure and increased temperature.

A batch of UHPC was prepared for this study. The regular CEM I PÇ 42.5R produced by Nuh cement company was used as cement material in the mix. Two different steel fibers, OL 6/16 and Dramix ZP 305 were added into the mix. Dramix ZP 305 steel fibers with hooked ends were used in the mix at two percent (2%) by volume. The fibers in the mix were with a diameter of 0.55 mm, a length of 30 mm and tensile strength of 1100 MPa. The short ones, OL 6/16, were straight fibers without hooked ends as meso fibers, 6 mm in length and 0.16 mm in diameter. The tensile strength of OL 6/16 steel fibers was 2250 MPa. Water-binder (cement + silica fume) ratio was kept constant at 0.14. The typical mix composition of the UHPC is given in Table 1.

Standard cubical (150 mm) concrete samples were tested in accordance to Turkish Standard TS EN 206 and TS EN 12390 to determine the compressive strength. Cubical samples were tested at a loading rate of 250 kN/min. The mean compressive strength of the concrete (f_{cm}) at the time of test was 152 MPa for cubical samples.

2.2 Steel properties

All the steel tubes were manufactured from mild steel by the steel company. In order to determine the actual material properties, three coupons were cut from each steel tube with different steel tube thickness according to Turkish Standard TS 138 EN 10002. The nominal outer dimensions of the all square hollow steel sections were 80 mm × 80 mm. The nominal steel tube thicknesses were selected as 2.5 mm, 3 mm and 4 mm. The average yield stress, tensile strength, and modulus of elasticity for each steel tube thickness are given in Table 2.

Table 2 The average steel tube material properties

	Yield strength (MPa)	Ultimate strength (MPa)	Modulus of elasticity (MPa)
2.5 mm steel tube thickness	288	385	200000
3 mm steel tube thickness	277	380	200000
4 mm steel tube thickness	268	367	200000

2.3 Preparation of the specimens

All specimens were 1300 mm in length and the nominal height-to-thickness ratio (H/t) of the specimens varied from 20 and 32. Hollow steel tubes were kept in an upright position in the stand specially prepared for the casting of the specimen. The insides of the hollow steel tubes were wire brushed to remove any rust and loose debris present. The deposits of grease and oil, if any, are cleaned away. The bottom ends of the hollow steel tubes were capped with 10 mm square steel base plate and the concrete is poured from the top. Concrete was filled in the hollow steel tubes in approximately five (300 mm) equal layers and each layer was compacted with 30 blows from a steel rod. The top of the concrete was trimmed off using a trowel and the concrete-filled hollow steel tubes were kept under the wet hessians for two weeks. The view of the UHPC-filled HSS



Fig. 1 The view of the UHPC-filled HSS beams

Table 3 The measured geometrical and material properties of the specimens

	$H \times B$ (mm \times mm)	t (mm)	L (mm)	$f_{cm,cube}$ (MPa)	f_y (MPa)	MOMENT (kN.m)
BF2.5-1	80.11 \times 80.04	2.51	1200	150.2	288	9.92
BF2.5-2	80.18 \times 80.13	2.51	1200	150.2	288	10.42
BF2.5-3	80.06 \times 80.17	2.52	1200	150.2	288	9.26
BH2.5-1	80.12 \times 80.15	2.49	1200	150.2	288	5.94
BH2.5-2	80.14 \times 80.11	2.49	1200	150.2	288	5.47
BF3-1	80.08 \times 80.13	3.02	1200	152.3	277	10.67
BF3-2	80.06 \times 80.12	3.04	1200	152.3	277	10.90
BF3-3	80.07 \times 80.15	3.01	1200	152.3	277	11.21
BH3-1	80.05 \times 80.09	2.98	1200	152.3	277	7.11
BH3-2	79.93 \times 80.19	2.99	1200	152.3	277	6.29
BF4-1	79.97 \times 80.14	4.04	1200	154.1	268	18.13
BF4-2	80.12 \times 80.09	4.03	1200	154.1	268	17.03
BF4-3	79.98 \times 80.11	4.02	1200	154.1	268	17.35
BH4-1	80.11 \times 80.02	3.99	1200	154.1	268	10.57
BH4-2	80.09 \times 80.06	4.02	1200	154.1	268	12.58

beams is shown in Fig. 1.

The specimens were labeled according to unfilled or filled of the steel tube, the thickness of steel tube and their order. For instance, BF2.5-1 denotes that the specimen is beam 'B', filled 'F', '2.5' the thickness of the steel tube, and '1' is the first specimen in this group. BH2.5-2, it is denoted 'B' beam, 'H' hollow steel tube, '2.5' the thickness of the steel tube, and '2' is the second specimen in this group. The geometrical and material properties are given in Table 3. The moment capacities of the HSS beams obtained from the test results are also given in Table 3.

2.4 Test set up and procedure

The specimens were tested in a 5000 kN capacity INSTRON testing machine. The tested beams were statically loaded to failure. The beams were tested under two-point loading applied at the centre of a very rigid plate to ensure the load distribution.

All beam specimens were a span length of 1200 mm and placed in simply supported by 50 mm diameter steel rods. The ratio of shear span to depth of the steel tube (a/D) was taken 5.6. At each load increment, the strain readings and the deflection measurements were recorded. The specimens were reached ultimate moments with no signs of lateral movement of the cross-section or any other

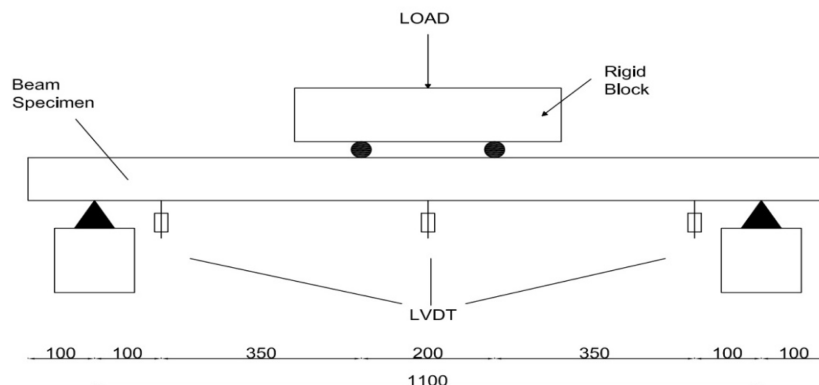


Fig. 2 The view of the Test set up



Fig. 3 The view of the BF3-1 under four-point bending at the test time

instability form. Four linear variable differential transducers (LVDT_s) were placed under the supports and mid-span of the beams to measure the deflections. Two strain gauges were used for each specimen to measure strains at the middle height, two strain gauges at the top and two strain gauges at the bottom. The test set up is shown in Fig. 2 and Fig. 3.

3. Results and discussion

3.1 Moment carrying capacity and curvature of the specimens

UHPC filled square hollow steel tube beams under flexure exhibited in a relatively ductile manner and significant increase in moment carrying capacity due to concrete filling of the hollow sections. Typical load (P)-mid-span deflections (Δ) and moment (M) - curvature (Φ) graphs are shown in Figs. 4-9. The moment-curvature diagrams showed that there is an initial elastic response, then inelastic behavior with gradually decreasing stiffness, until the ultimate moment is reached asymptotically.

3.2 Performance indices

Relative Ductility Index (RDI) that represents the increase in ductility of the UHPC-filled HSS beams compared with the hollow tubes is defined in Eq. (2). As shown in Figs. 7-9, the ductility of

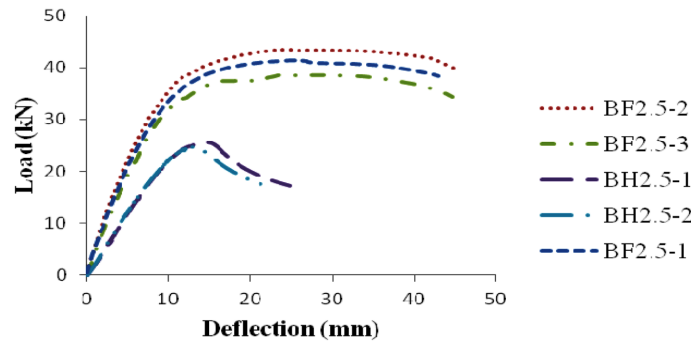


Fig. 4 Load vs. mid- span deflection of beam specimen with 2.5 mm steel tube wall

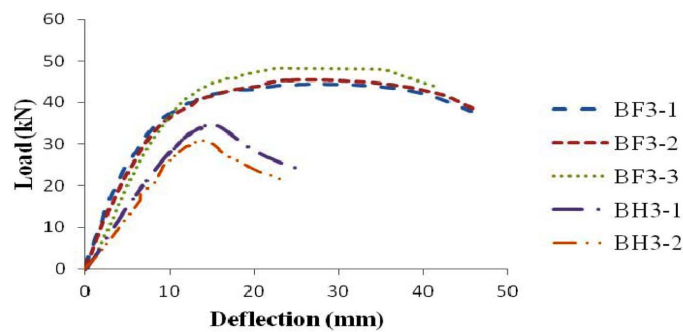


Fig. 5 Load vs. mid- span deflection of beam specimen with 3 mm steel tube wall

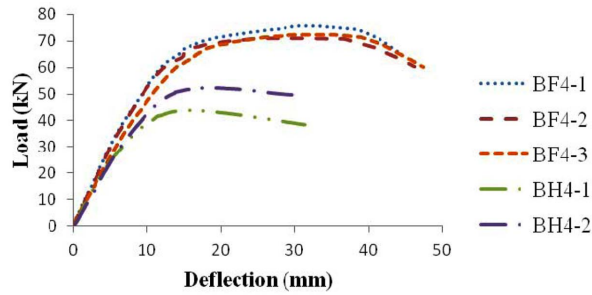


Fig. 6 Load vs. mid-span deflection of beam specimen with 4 mm steel tube wall

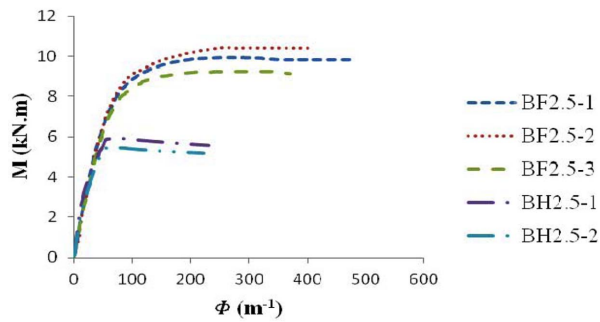


Fig. 7 Moment (M) vs.-curvature (Φ) relations of the beam specimens with 2.5 mm steel tube wall

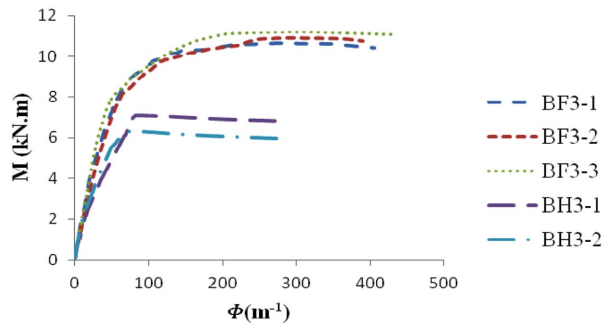


Fig. 8 Moment (M) vs.-curvature (Φ) relations of the beam specimens with 3 mm steel tube wall

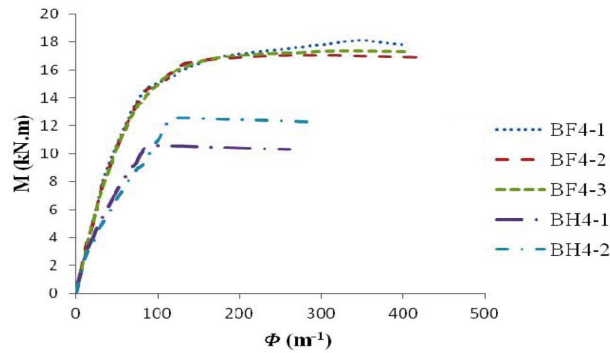


Fig. 9 Moment (M) vs.-curvature (Φ) relations of the beam specimens with 4 mm steel tube wall

Table 4 Ultimate moment capacity, curvature, and performance indices of the UHPC-filled HSS beams

	$H \times B$ (mm \times mm)	t (mm)	MOMENT (kNm)	CURVATURE	RDI	SIF
BF2.5-1	80.11 \times 80.04	2.51	9.92	258	4.16	1.74
BF2.5-2	80.18 \times 80.13	2.51	10.42	263	4.24	1.83
BF2.5-3	80.06 \times 80.17	2.52	9.26	229	3.69	1.62
Avg.			9.87			
St. Dev.			0.58			
BF3-1	80.08 \times 80.13	3.02	10.67	272	3.47	1.59
BF3-2	80.06 \times 80.12	3.04	10.90	284	3.64	1.62
BF3-3	80.07 \times 80.15	3.01	11.21	291	3.73	1.67
Avg.			10.93			
St. Dev.			0.27			
BF4-1	79.97 \times 80.14	4.04	18.13	344	3.37	1.56
BF4-2	80.12 \times 80.09	4.03	17.03	306	3	1.47
BF4-3	79.98 \times 80.11	4.02	17.35	322	3.16	1.5
Avg.			17.5			
St. Dev.			0.57			

the hollow specimens is increased due to concrete filling and the increase in the steel tube thickness.

$$RDI = \frac{\Phi_{CFT}}{\Phi_{Hollow}} \quad (1)$$

Strength Increasing Factor (SIF) that represents the increase in ultimate moment capacity of the UHPC-filled HSS beams compared with the hollow tubes is defined in Eq. (3).

$$SIF = \frac{M_{CFT}}{M_{Hollow}} \quad (2)$$

Here, M_{CFT} is the experimental moment capacity of concrete-filled hollow steel sections; M_{Hollow} is the experimental moment capacity of the hollow steel tubes. It was found that the maximum advantage (M_{CFT}/M_{Hollow}) of filling is obtained for tubes with lower wall thickness of the concrete-filled HSS. This significant increase in moment capacity is mainly due to thinner sections are more susceptible to local buckling compared with the thicker ones. Concrete filling into the thinner hollow steel sections helps in delaying the local buckling and hence enhance the moment carrying capacity of the specimens. The performance indices, moment capacities and corresponding curvatures of all specimens obtained from the tests are given in Table 4.

The performance indices values of RDI and SIF obtained in this study were compared with the results of (Chitawadagi and Narasimhan 2009) with nominal concrete strength 20, 30 and 40 MPa. The comparison of the performance indices values are shown in Fig. 10.

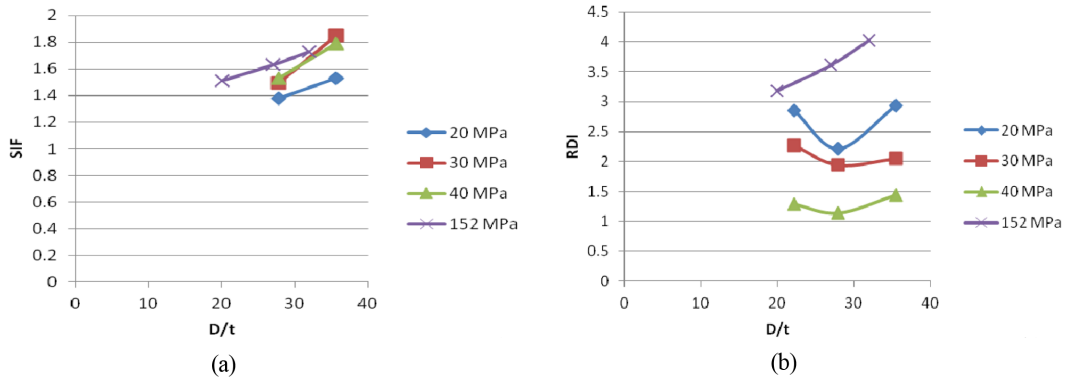


Fig. 10 Comparison of RDI and SIF with different concrete strength (a) SIF- D/t relationship, (b) RDI- D/t relationship

3.3 Comparison of moment capacities with design codes

The moment capacities obtained from the test results were compared with the design codes such as Eurocode 4, AISC-LRFD, CIDECT and L.H. Han model.

3.3.1 Eurocode 4

In Eurocode 4, the resistance of a composite column subjected to combined compression and bending is determined from an interaction curve. An interaction curve between compressive axial load and moment can be obtained for a short composite column by considering several possible

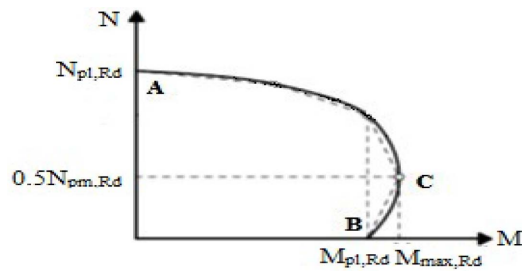


Fig. 11 Interaction curve for linear approximation

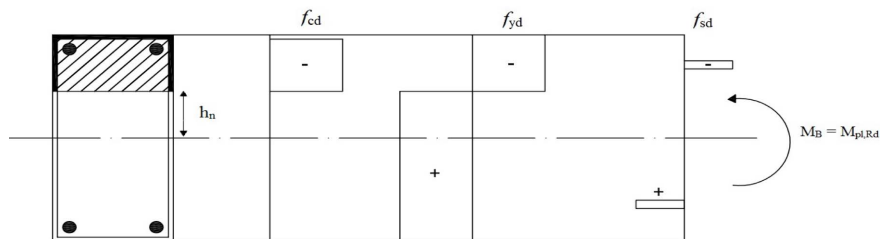


Fig. 12 Stress distributions for the B point on the interaction curve for concrete filled hollow sections, according to the Eurocode 4

positions of the neutral axis with the cross-section, and determining the internal forces and moments from the resulting plastic stress blocks. As shown in Fig. 11 and Fig. 12, for the simplified method given within Eurocode 4, Point B corresponds to the plastic moment resistance of the cross-section, in the absence of an applied axial load.

$$\begin{aligned} N_B &= 0 \\ M_B &= M_{pl, Rd} \end{aligned}$$

$$M_{pl, Rd} = f_{yd}(W_{pa} - W_{pan}) + 0.5f_{cd}(W_{pc} - W_{pcn}) + f_{sd}(W_{ps} - W_{psn}) \quad (3)$$

$$W_{pc} = \frac{(b-2t)(h-2t)^2}{4} - \frac{2}{3}r^3 - r^2(4-\pi)\left(\frac{h}{2} - t - r\right) - W_{ps} \quad (4)$$

$$h_n = \frac{A_c f_{cd} - A_{sn}(2f_{sd} - f_{cd})}{2bf_{cd} + 4t(2f_{yd} - f_{cd})} \quad (5)$$

$$W_{pan} = 2th_n^2 \quad (6)$$

$$W_{pcn} = (b-2t)h_n^2 - W_{psn} \quad (7)$$

Here h_n is distance from the centre-line of the composite cross-section to the compression region. W_{pa} , W_{pc} , W_{ps} are the plastic section modulus for the steel section, the concrete of the composite cross-section and the reinforcement ($W_{ps} = 0$ for this study), respectively.

W_{pan} , W_{pcn} , W_{psn} are the plastic section modulus of the corresponding components within the region of $2h_n$ from the centre-line of the composite cross-section.

3.3.2 AISC-LRFD

The flexural strength of the CFSHS columns according to the AISC-LRFD was determined based only on the steel hollow section. The plastic moment resistance of a concrete filled hollow section may be evaluated as follows

$$M_{AISC} = Zf_y \quad (8)$$

Here Z and f_y is the plastic section modulus and yield strength of the hollow steel tube, respectively.

3.3.3 CIDECT

The ultimate moment capacity for concrete-filled steel hollow sections according to the CIDECT can be defined as in Eq. (9).

$$M_{u, CIDECT} = M_{ratio} \frac{D^2 B - (D-2t)^2 (B-2t) f_y}{4} \quad (9)$$

Here M_{ratio} is a ratio of the bending capacity of composite hollow section to that of the hollow section, D is the depth of the composite section, B is the width of the composite section, t is the thickness of the composite section and f_y is the yield stress of the steel tube.

3.3.4 Han (2004) model

According to Han (2004), the moment capacity of the composite beams is given by the following equations.

$$M_u = \gamma_m f_{scy} W_{scm} \quad (10)$$

$$f_{scy} = (1.18 + 0.85 \xi) \cdot f_{ck} \quad (11)$$

$$W_{scm} = \frac{B^3}{6} \quad (12)$$

$$\xi = \frac{A_s f_{yk}}{A_c f_{ck}} \quad (13)$$

$$\gamma_m = 1.04 + 0.48 \ln(\xi + 0.1) \quad (14)$$

Here, M_u is the moment capacity of the composite section; f_{scy} is the nominal yielding strength of the composite sections, W_{scm} is the section modulus of composite section, ξ is the constraining factor, and γ_m is the flexural strength index. Comparisons between test results and the design codes are shown in Table 5.

Table 5 Comparison of experimental moment capacities values with design codes and Han model

	M_{Test} (kNm)	M_{EC4}	$M_{EC4}/$ M_{Test}	M_{AISC}	$M_{AISC}/$ M_{Test}	M_{CIDECT}	$M_{CIDECT}/$ M_{Test}	M_{Han}	$M_{Han}/$ M_{Test}
BF2.5-1	9.92	6.71	0.68	5.96	0.60	10.9	1.10	10.1	1.02
BF2.5-2	10.42	6.71	0.64	5.96	0.57	11.4	1.09	10.1	0.97
BF2.5-3	9.26	6.71	0.72	5.96	0.64	10.2	1.10	10.2	1.10
Avg.			0.68		0.6		1.10		1.03
St.Dev.			0.04		0.04		0.01		0.07
BF3-1	10.67	7.72	0.72	7.13	0.67	11.6	1.09	11.5	1.08
BF3-2	10.90	7.73	0.71	7.13	0.65	12.0	1.10	11.6	1.06
BF3-3	11.21	7.72	0.69	7.13	0.64	12.9	1.15	11.5	1.03
Avg.			0.71		0.65		1.11		1.06
St.Dev.			0.02		0.02		0.03		0.03
BF4-1	18.13	9.5	0.52	9.04	0.50	14.6	0.81	14.5	0.80
BF4-2	17.03	9.5	0.56	9.04	0.53	13.7	0.80	14.5	0.85
BF4-3	17.35	9.49	0.55	9.04	0.52	13.9	0.80	14.5	0.84
Avg.			0.54		0.52		0.8		0.83
St.Dev.			0.02		0.02		0.01		0.03
Avg. (all samples)			0.64		0.59		1		0.97
St. Dev.(all samples)			0.08		0.06		0.15		0.11

4. Conclusions

Results of experimental investigations of square hollow and UHPC-filled HSS beams have been presented in this paper. The following conclusions are highlighted.

A significant increase in the moment capacity and the corresponding curvature of all the hollow sections used in this study are observed due to concrete filling.

An increase in the wall thickness of the steel tube increases the ultimate moment capacity and the corresponding curvature both the hollow and UHPC-filled HSS beams. However, the increase in the moment capacity and the corresponding curvature is much greater for thinner HSS beams than thicker ones. From Table 4, it can be seen that if the steel tube thickness of the HSS beams is reduced from 4 mm to 2.5 mm, there is a significant increase in the values of RDI and SIF. This significant increase in the moment capacity and the corresponding curvature is primarily because of the thinner sections are more vulnerable to local buckling as compared to thicker ones. Therefore, the design codes may consider the height-to-thickness ratio (H/t) of the HSS beams as well as the compressive strength of the concrete or the yield strength of the steel section to calculate the moment capacity of the HSS beams.

From Fig. 10, when we compare the values of SIF and RDI with the results of Chitawadagi and Narasimhan (2009), it is observed that although there is a substantial increase in relative ductility index (RDI) due to an increase in the strength of in-filled concrete, there is no appreciable increase in strength increasing factor (SIF).

Eurocode 4 and AISC-LRFD predict the ultimate moment capacity of the all UHPC-filled HSS beams conservatively. However, both of these design codes are safer for the thinner HSS beams than thicker ones. The AISC-LRFD, to obtain good convergence in experimental results, should take into account the effects of concrete in-fill calculating the moment capacity of the HSS beams. Furthermore, these design codes are more successful to predict the ultimate moment capacity than CIDECT design code and Han model.

Although the CIDECT design code and Han model are conservative for thicker HSS beams, they slightly overestimate the ultimate moment capacity of the UHPC-filled HSS beams with thinner ones.

References

- AISC-LRFD (1999), "Load and resistance factor design specification for structural steel buildings", American Institute of Steel Construction.
- Arivalagan, S. and Kandasamy, K. (2009), "Energy absorption capacity of composite beams", *J. Eng. Sci. Technol. Rev.*, **2**, 145-150.
- Chitawadagi, M.V. and Narasimhan, M.C. (2009), "Strength deformation behavior of circular concrete filled steel tubes subjected to pure bending", *J. Constr. Steel Res.*, **65**, 1836-1845.
- CIDECT (1995), J. Wardenier, D. Dutta, N. Yeomans, J.A. Parker, O. Bucak: Design Guide for Structural Hollow Sections in Mechanical Applications, CIDECT, Construction with Hollow Steel Sections, Verlag TUV Rheinland GmbH, Köln.
- Elchalakani, M., Zhao, X.L. and Grzebieta, R.H. (2001), "Concrete-filled circular steel tubes subjected to pure bending", *J. Constr. Steel Res.*, **57**, 1141-1168.
- Eurocode 4 EN 1994-1-1, "Design of composite steel and concrete structures Part 1.1: General rules and rules for buildings".
- Han, L.H. (2004), "Flexural behavior of concrete-filled steel tubes", *J. Constr. Steel Res.*, **60**, 313-337.

- Gho, W. and Liu, D. (2004), "Flexural behavior of high-strength rectangular concrete-filled steel hollow sections", *J. Constr. Steel Res.*, **60**, 1681-1696.
- Kong, J.Y., Choi, E.S., Chin, W.J. and Lee, J.W. (2007), "Flexural behavior of concrete-filled steel tube members and its application", *Steel Struct.*, **7**, 319-324.
- Kim, Y.H., You, S.K., Jung, J.H. and Yoon, S.J. (2006), "Strengthening effect of the shear key on the flexural behavior of concrete filled circular tube", *Steel Struct.*, **6**, 183-190.
- Lu, Y.Q. and Kennedy, D.J.L. (1994), "The flexural behavior of concrete-filled hollow structural sections", *Canadian J. Civil Eng.*, **21**, 11-130.
- Nakamura, S., Hosaka, T. and Nishiumi, K. (2004), "Bending behavior of steel pipe girders filled with ultralight mortar", *J. Bridge Eng.*, **9**(3), 297-303.
- Probst, A.D., Thomas, H., Kong, K., Ramseyer, C. and Kim, U. (2010), "Composite flexural behavior of full-scale concrete-filled tubes without axial loads", *J. Struct. Eng., ASCE*, **136**, 1401-1412.
- Prion, H.G.L. and Boehme, J. (1994), "Beam-column behavior of steel tubes filled with high strength concrete", *Can. J. Civil Eng.*, **21**, 207-218.
- Shawkat, W. and Fahmy, W. (2008), "Cracking patterns and strength of CFT beams under different moment gradients", *Compos. Struct.*, **84**, 159-166.
- Soundararajan, A. and Shanmugasundaram, K. (2008), "Flexural behaviour of concrete-filled steel hollow sections beams", *J. Civil Eng. Manage.*, **14**, 107-114.
- TS EN 206 (2002), Concrete-Part 1: Specification, Performance, Production and Conformity, Turkish Standard Institution, Ankara.
- TS EN 12390 (2002), Testing Hardening Concrete- Part 1, Shape, Dimensions and Other Requirements for Specimens and Moulds, Turkish Standard Institution, Ankara.
- TS 138 EN 10002-1 (2004), Metallic materials – Tensile testing –Part 1, Method of test at ambient temperature, Turkish Standards Institution, Ankara.
- Varma, A.H., Ricles, J.M., Sause, R. and Lu, L.W. (2002), "Seismic behavior and modeling of high-strength composite concrete-filled steel tube (CFT) beam-columns", *J. Constr. Steel Res.*, **58**, 725-758.

Notations

A_c	: Cross-sectional area of the concrete core
A_s	: Cross sectional area of the steel tube
D	: Outer diameter of the steel tube
B	: Outer width of the steel tube
$f_{cm,cube}$: The mean compressive strength of the cube samples at the test time
f_{ck}	: Characteristic compressive strength of concrete
f_y	: Yield stress of the steel tube
f_{scy}	: Nominal yielding strength of the composite section
W_{scm}	: The section modulus of composite section